

Optomechanical design concept for GMACS, a wide-field, multi-object, moderate resolution optical spectrograph for the Giant Magellan Telescope (GMT)

Stephen A. Smee^{*a}, Travis Prochaska^b, Stephen A. Sackett^c, Randolph P. Hammond^a, Robert H. Barkhouser^a, D. L. DePoy^b, J. L. Marshall^b

^aDept. of Physics and Astronomy, Johns Hopkins University, Baltimore, MD, 21218 (USA)

^bDept. of Physics and Astronomy, Texas A&M University, College Station, TX, 77843 (USA)

^cObservatories of the Carnegie Institution for Science, Pasadena, CA, 91101, (USA)

ABSTRACT

We describe the conceptual optomechanical design for GMACS, a wide-field, multi-object, moderate-resolution optical spectrograph for the Giant Magellan Telescope (GMT). GMACS is a candidate first-light instrument for the GMT and will be one of several instruments housed in the Gregorian Instrument Rotator (GIR) located at the Gregorian focus. The instrument samples a 9 arcminute x 18 arcminute field of view providing two resolution modes (i.e. low resolution, $R \sim 2000$, and moderate resolution, $R \sim 4000$) over a 3700 Å to 10200 Å wavelength range. To minimize the size of the optics, four fold mirrors at the GMT focal plane redirect the full field into four individual “arms”, that each comprises a double spectrograph with a red and blue channel. Hence, each arm samples a 4.5 arcminute x 9 arcminute field of view. The optical layout naturally leads to three separate optomechanical assemblies: a focal plane assembly, and two identical optics modules. The focal plane assembly contains the last element of the telescope’s wide-field corrector, slit-mask, tent-mirror assembly, and slit-mask magazine. Each of the two optics modules supports two of the four instrument arms and houses the aft-optics (i.e. collimators, dichroics, gratings, and cameras). A grating exchange mechanism, and articulated gratings and cameras facilitate multiple resolution modes. In this paper we describe the details of the GMACS optomechanical design, including the requirements and considerations leading to the design, mechanism details, optics mounts, and predicted flexure performance.

Keywords: spectrograph, camera, CCD, VPH grating

1. INTRODUCTION

We present the optomechanical design of the Wide Field, Multi-Object, Moderate-Resolution, Optical Spectrograph (called GMACS) for the GMT.¹ GMACS is an instrument capable of observing the faintest possible targets, those that are substantially fainter than the sky. High throughput, simultaneous wide wavelength coverage, accurate and precise sky subtraction, moderate resolution, and wide field (for an extremely large telescope) are the crucial design drivers for the instrument. We expect that GMACS will form one of the most basic scientific capabilities of the GMT.

The conceptual mechanical design of GMACS has two basic sub-systems: a focal plane unit that translates into the active space in the Gregorian Instrument Rotator (GIR) and is lifted to the telescope focal plane via an elevator mechanism, and a set of optics modules that contain the individual arms and channels. The focal plane unit is stored in the lower half of one GIR bay; the optics modules are permanently fixed to the “ceiling” of the GIR and occupy the top half of two bays (separated by 180 degrees). Each is described in additional detail below. Figure 1 shows the locations of these sub-systems in the GIR.

* smee@pha.jhu.edu; phone 410-516-7097; fax 410-516-6664; <http://idg.pha.jhu.edu>

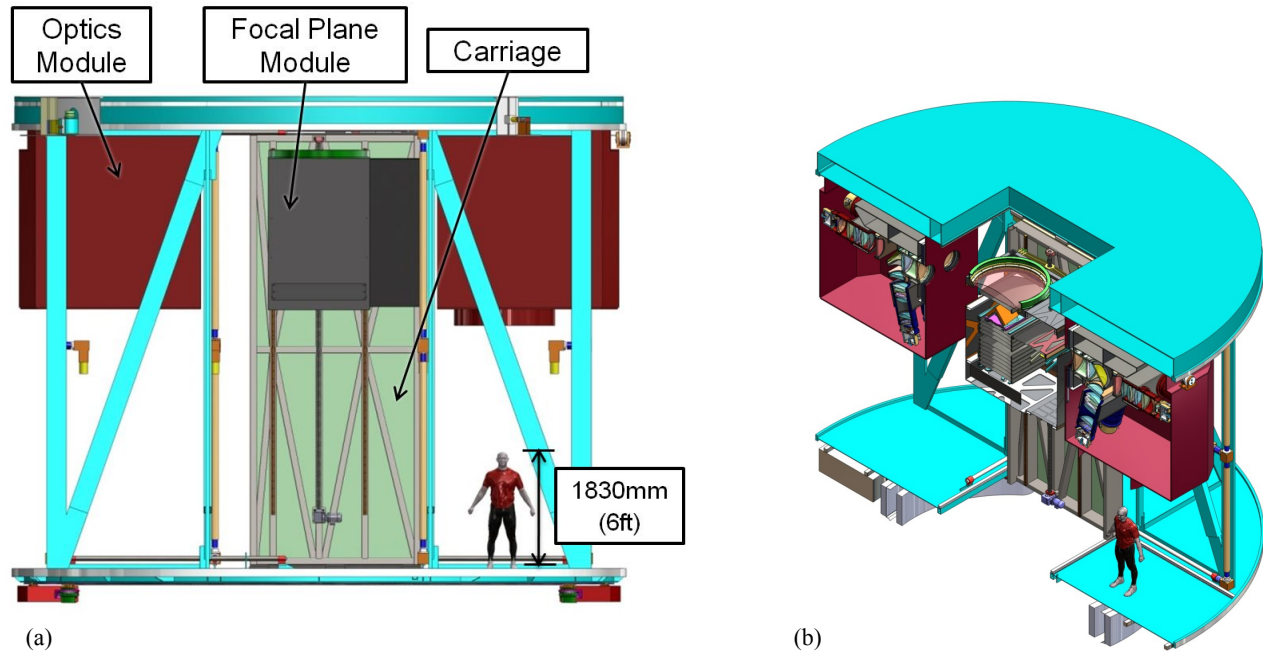


Figure 1 (a) Side view of the Gregorian Instrument Rotator showing the various sub-systems in the aligned and ready-to-observe position. A rendered image of a six foot tall man is given for scale. And (b), Section view of the GIR with GMACS installed.

2. FOCAL PLANE UNIT

Figure 2 shows the focal plane unit with associated sub-assemblies. The focal plane unit holds and positions the final element of the GMT wide-field corrector lens, slit mask, and tent mirrors in optical alignment relative to the telescope and optics modules. The focal plane unit also contains a magazine of slit masks that will be used during the night. Up to 12 slit masks can be held ready for observing. The unit also holds the electronics to control and use the accompanying mechanisms.

2.1 The Focal Plane Unit Carriage

The carriage will conform to the GIR standard for translation stages established by GMT. This will provide for lateral motion from the storage position into the observing position. An additional motion upwards to put the focal plane unit at the main focus of the telescope will also be required.

An elevator mechanism integral to the carriage lifts the entire focal plane unit into position once the carriage is translated to the focal plane position. The elevator mechanism consists of two linear THK rails to guide the focal plane unit. A drive motor and gear reducer coupled to a precision ball nut provides the motive force. The total travel range is 3000 mm.

2.2 The field lens mount

The focal plane unit will contain a cell for the last element of the corrector. The cell will be made from aluminum and will have radial, spring-loaded supports to account for coefficient of thermal expansion (CTE) differences between the glass and aluminum housing. The lens is expected to be 1393 mm in diameter and weigh roughly 426 kg, so the cell will need careful design and analysis to guarantee optical alignment is maintained for all telescope pointing angles and temperature extremes. We anticipate working closely with GMT to ensure appropriate tolerances are understood and maintained.

2.3 The tent mirror assembly

The tent mirrors quarters the FOV and directs the resulting portions to the appropriate collimators. Instrument focus will be provided by a set of three actuators on the back of each mirror; these could also be used for flexure compensation. The assembly includes four, identical, Zerodur mirrors. Each mirror fits within a 605 x 370 x 60 mm envelope and has a mass of 29 kg. The entire assembly is affixed to the field lens bench and has a mass of 286 kg. Four pads are bonded to each mirror. The central pad mates to a membrane flexure and the peripheral pads pre-load the mirror to the bench and provide tip/tilt adjustment. Figure 3 shows additional detail on the bond pads and flexure.

2.4 The slit mask exchange mechanism

Individual slit masks ride on rails and are inserted into the observing position with a linear actuator; see Figure 4. The slit masks are captured kinematically and will be held in place with a stability of ~ 10 microns, which corresponds to ~ 0.01 arcsec. The slit masks are a minimum of 527 mm x 1145 mm in extent; we currently anticipated that each mask will have a cartridge that will be 1286 mm x 860 mm x 80 mm; the masks will be curved to follow the best focal surface of the telescope. The masks will ride on rails as inserted into the storage and observing locations. The top sets of rollers that guide the cartridges into location will have eccentric shafts to set distance between sets of rollers & guide wheels. Rollers are used on the right to keep the slit mask from being over-constrained. While translating, the tracks will remain in contact with at least 2 pairs of guide wheels at any time. The slit mask magazine holds as many as 12 slit masks and the slit mask elevator moves the slit masks from the magazine to the observing position. The mask elevator uses two linear motions and a rotating motion to move the mask from the magazine to the focal plane. The rotating motion engages a detent on the mask cartridge. A horizontal linear motion extracts the mask from the magazine, and vertical linear motion raises the mask to the height of the focal plane where the mask is inserted beneath the field lens (i.e., the last element of the corrector).

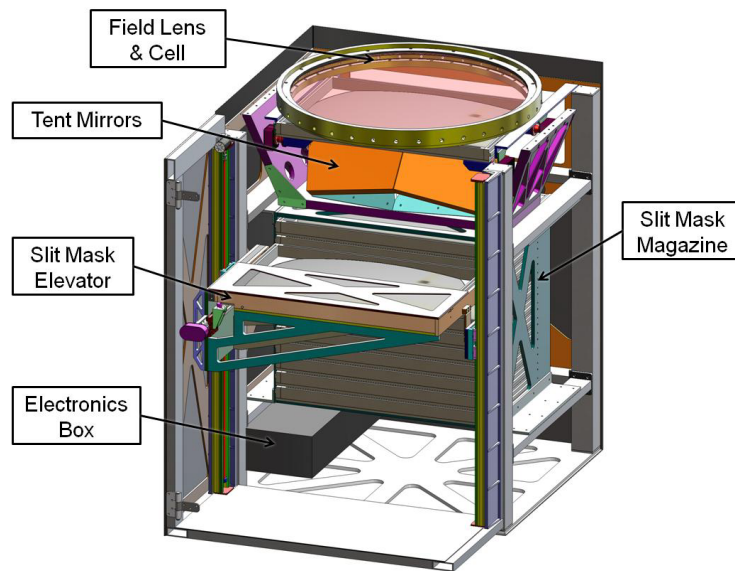


Figure 2 Focal plane unit and labeled sub-assemblies. This unit moves laterally into the active space for observing in the GIR and then is lifted into final position on an internal elevator.

2.5 Acquisition and alignment cameras

The focal plane unit also carries four alignment and acquisition cameras. These cameras are in a fixed location behind the focal plane and include a 4:1 re-imaging system. The re-imaging optics produce a scale of ~ 4 arcsec per mm or 0.06 arcsec per 15 μm pixel. We currently anticipate using a commercial 1024 x 1024 CCD system, thus we expect a field of view of roughly 1 arcminute x 1 arcminute at each of the four locations around the focal plane.

The acquisition and alignment cameras will be in fixed locations behind reference holes cut in every slit mask; one hole just outside of each corner of the tent mirror assembly. They will allow precision alignment of the slit masks relative to reference stars that can be positioned appropriately on the CCDs. The density of reference objects on the sky is very high, since the GMT can detect extremely faint objects very quickly. Specifically, for a CCD system with a permanently mounted DES-r filter (similar to SDSS r) we expect

$$S/N \approx 400 \frac{10^{20-m/2.5}}{(10^{20-m/2.5} + 0.4)^{1/2}}$$

where m is the brightness of a reference object in the DES-r band. We assume a system efficiency of ~ 0.5 , ~ 0.7 arcsec seeing, and ~ 20 mag/arcsec² sky brightness. For objects that have DES-r ≈ 24 mag, we expect a $S/N \approx 15$ in ~ 1 second exposures (it is worth remembering at this point that the GMT has a very large collecting area!). There are expected to be ~ 30 stars and galaxies of this brightness per arcminute² in the sky near the galactic cap; all of which will be imaged and catalogued by DES before GMT begins operations. Indeed, we may need to purposely limit the sensitivity of the alignment cameras so as to allow operation in the galactic plane, where source confusion would be severe.

The large number of objects that we will detect in very short exposures with the alignment and acquisition cameras convince us that fixed positions is adequate to align the slit masks in all three dimensions (right ascension, declination, and rotation angle). We also note that GMACS will have an imaging mode. Although the science case for the full imaging mode is not obvious, the mode will be useful for checking the co-alignment of the acquisition and alignment cameras with the instrument focal planes.

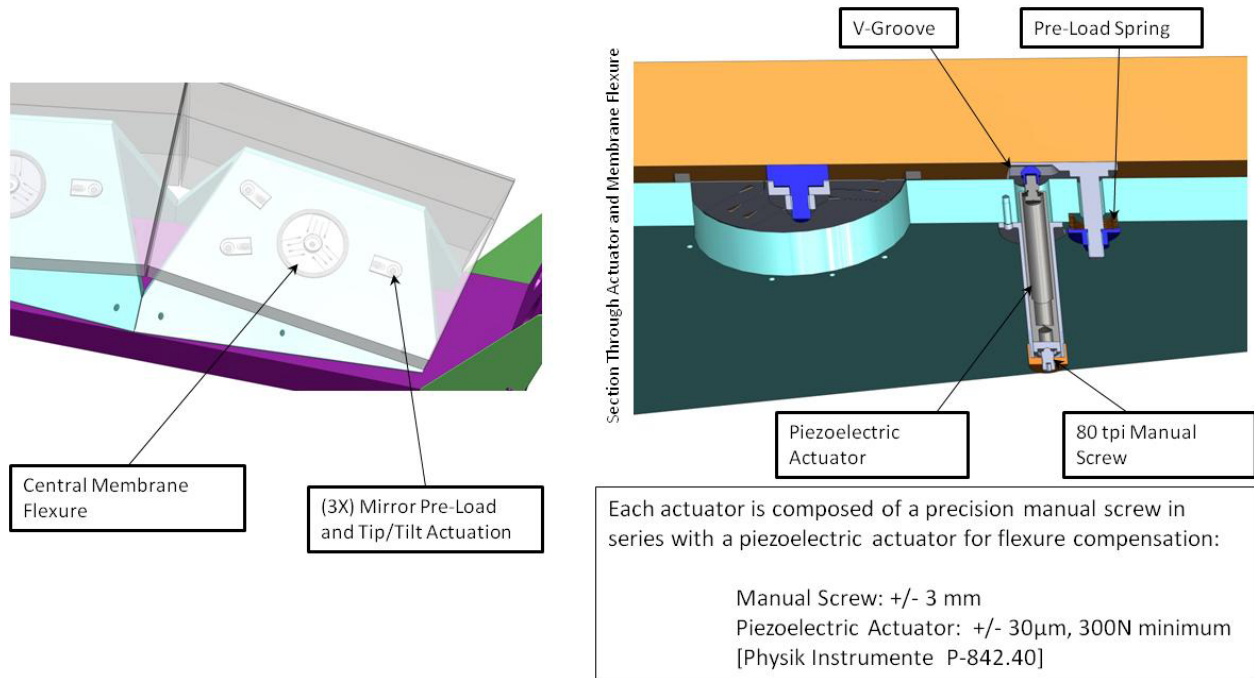


Figure 3 Tent mirror assembly detail showing details of the bond pads and membrane flexure support.

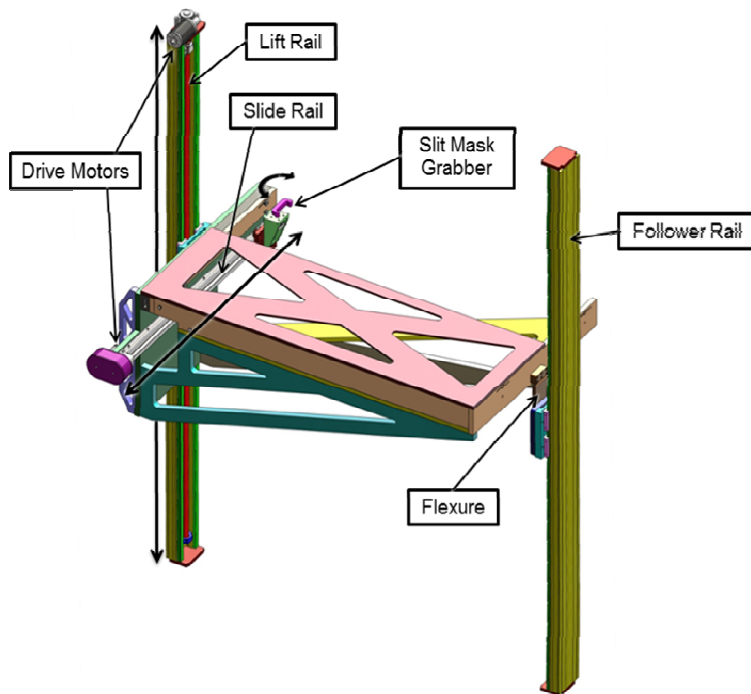


Figure 4 Rendering of the slit mask elevator.

3. OPTICS MODULES

The optics modules contain the spectrograph collimators, dichroics, gratings, and cameras and are attached via flexures to the “ceiling” of the GIR. Two optics modules collimate, disperse, and reimage the slit field. There are four arms total, two per module. The light is split in each arm into a red and blue channel. Each arm contains a collimator, a dichroic, four VPH gratings (low and high dispersion), a red camera, and a blue camera.

Both red cameras, as well as the two blue cameras, articulate as a pair to achieve different spectroscopic modes. The technical specifications require the instrument to have two resolutions per channel. For reference, we have adopted a low resolution ($R \sim 2000$) and a high resolution ($R \sim 4000$) capability for the fiducial design. This requires articulated cameras and a grating exchange mechanism. To simplify articulation and to do it in a way that is mechanically stiff, both red cameras and both blue cameras are articulated in pairs. Gratings from the two channels are also articulated as an ensemble. The “open” design does expose many optical surfaces to dust and debris, as well as stray light. We will need an environmental enclosure that surrounds the optics module. Aluminum is used throughout in order to minimize mass, maximize stiffness, and avoid CTE mismatches at critical interfaces.

We investigated other options in addition to the articulating camera structure. These were legacy from the original GMACS design and included a fixed camera-collimator angle and grisms to provide additional resolutions. We found that the grisms would be large and unwieldy and difficult to reconcile with a simple instrument structure; interchange of the grism units would be difficult and risky to valuable components. This approach would also constrain the wavelength coverage specific choices, which reduces potential rapid reconfiguration options and general observing flexibility.

Overall we feel the conceptual design of the instrument with articulating cameras and two grating interchange mechanism per channel is solid and that critical concepts have been developed. In particular the optical bench, camera and grating articulation mechanism, grating exchanger, and optics mounts all draw from previous design heritage and experience of the team. Figure 5 - Figure 7 show renderings of various views of the optics modules and give additional design details.

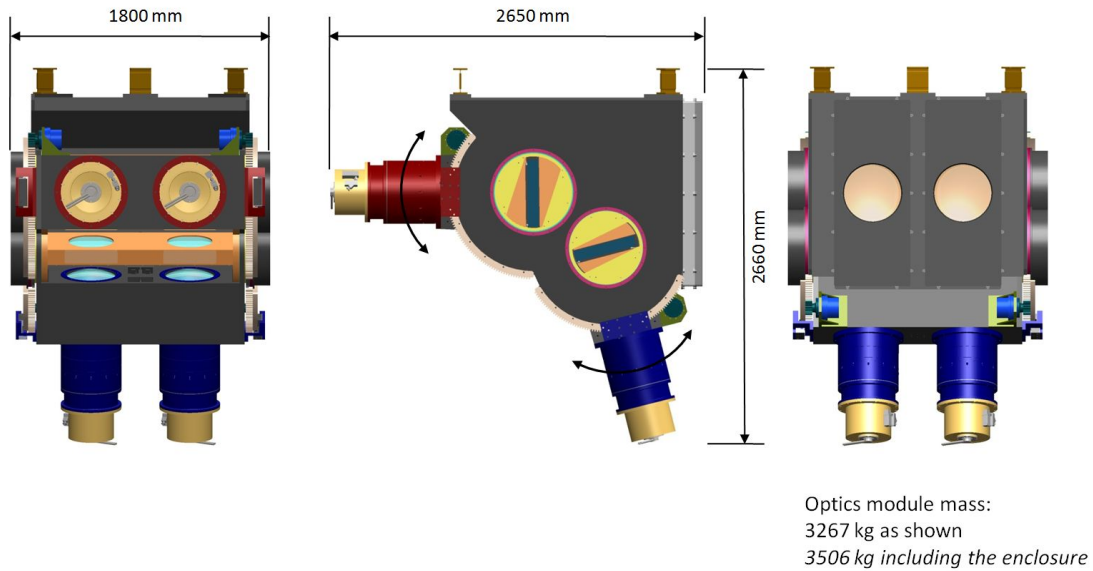


Figure 5 Back, side, and front views of the optics module. GMACS consists of two optics module in the full-field implementation.

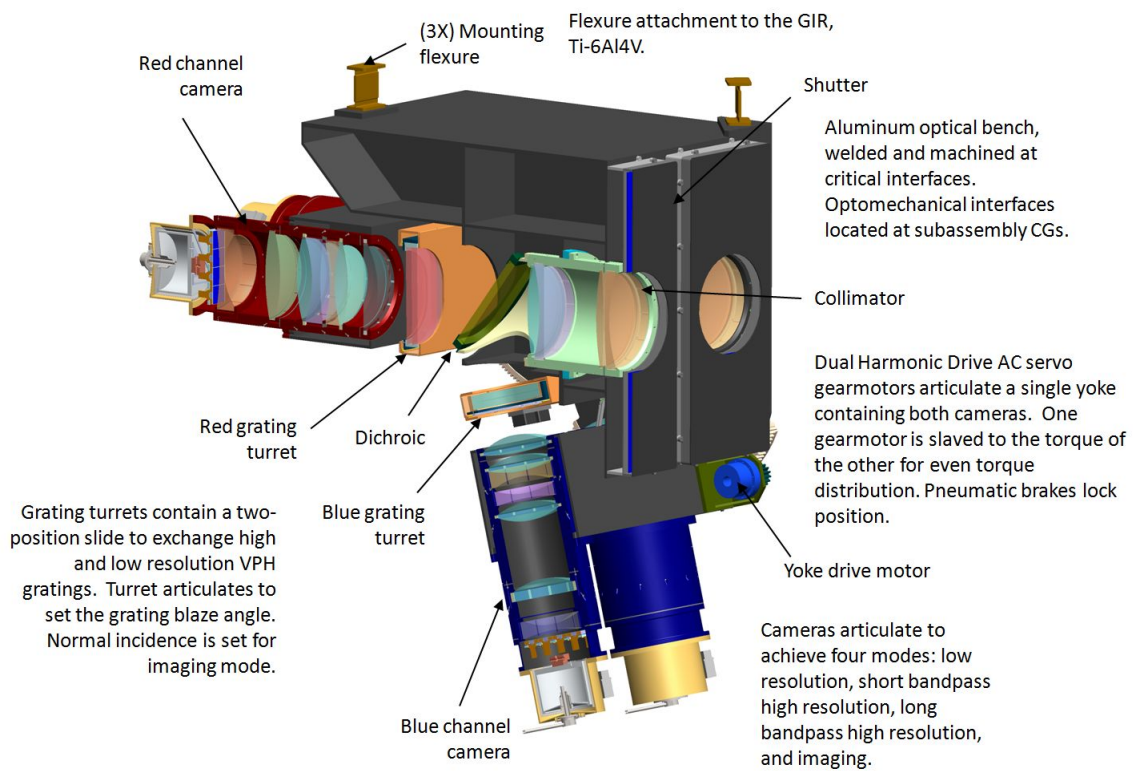


Figure 6 Cut-away view of the optics module with various details highlighted.

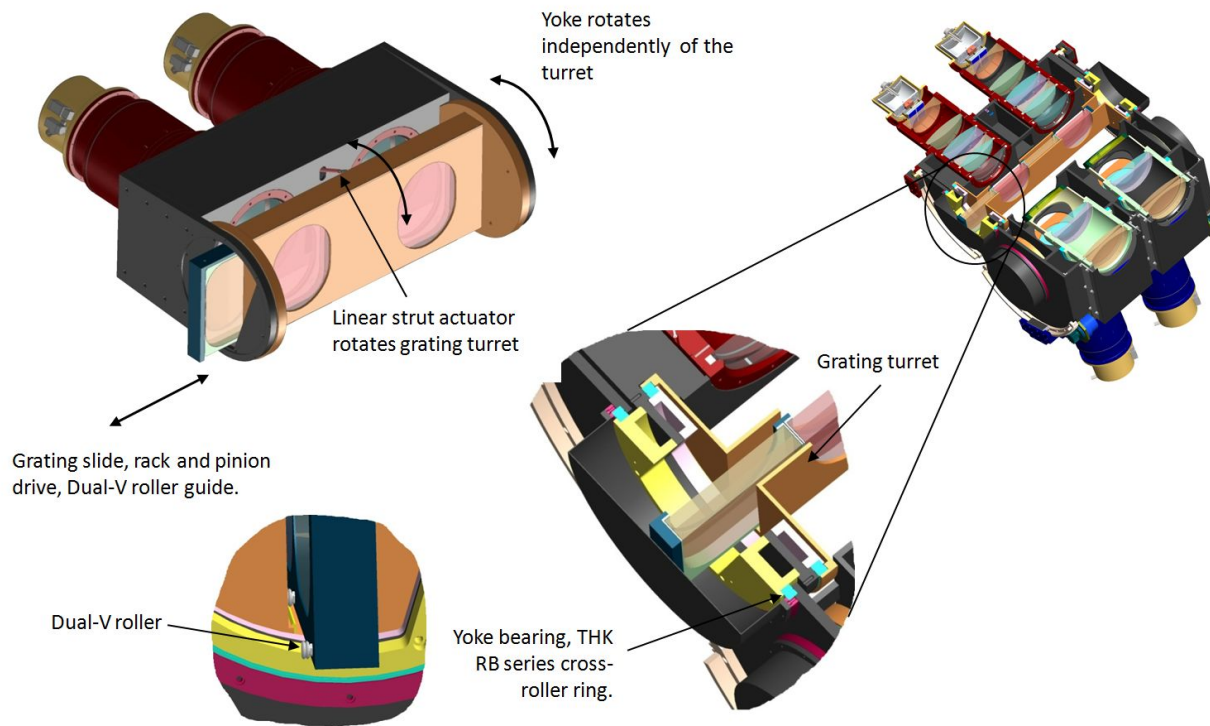


Figure 7 Renderings highlighting details of the yoke rotation mechanism and grating exchange mechanism.

3.1 The Yoke drive mechanism

The camera yoke rotates about two THK cross-roller ring bearings attached to the external faces of the optical bench. A Dual Harmonic Drive AC servo actuator model SHA 40A 161 with brake drives a 6 pitch spur gear against a mating arc gear. The torque is 841 Nm per drive, 1682 Nm total, 3.67x greater than required. One drive is slaved to the torque of the other for even loading. Pneumatic rail brakes, one on each arc gear, lock the yoke position allowing any orientation to be achieved within the limits of travel thus eliminating concerns about the effects of gear lash on flexure. Limit switches set the range of motion and additional limit switches prevent red/blue collision. There will also be hard stops to preclude over-travel.

3.2 Grating turret rotation

The grating turret rotates on two THK cross-roller ring bearings on the inside face of each yoke plate. Rotation is driven by an Ultramotion Digit HT17 linear strut actuator which provides simple backlash free motion. Encoding is not yet finalized, but options include linear potentiometer (baseline), an encoder on the bearing spool, or simply open loop operation.

3.3 Grating exchange mechanism

The grating drive has similar design principles as the other mechanisms. For example, limit switches set range of motion and hard stops preclude over-travel. Two sets of dual-V roller bearings ride on parallel tracks to provide the requisite linear motion. The motive force is provided by a rack and pinion drive.

3.4 Collimator and camera optomechanics

Figure 8, Figure 9, and Figure 10 show various details of the collimator assembly, the blue camera, and the red camera, respectively. The lens cell concepts shown are borrowed directly from the cells used in the FourStar infrared camera and the SDSS spectrographs, which are known to work well. These are incorporated into the optics modules.

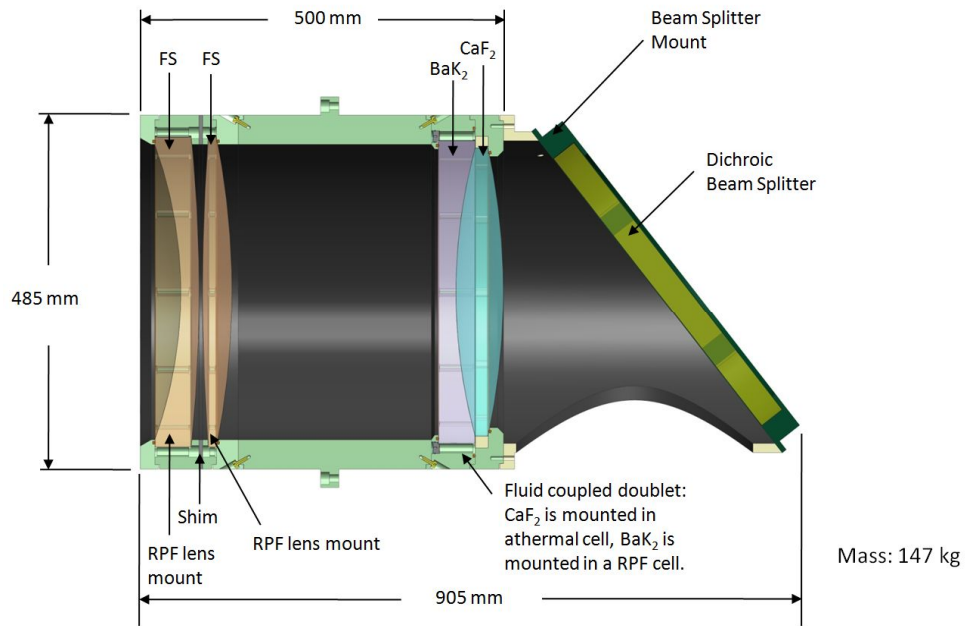


Figure 8 Section view of the collimator assembly with the dichroic beam splitter attached.

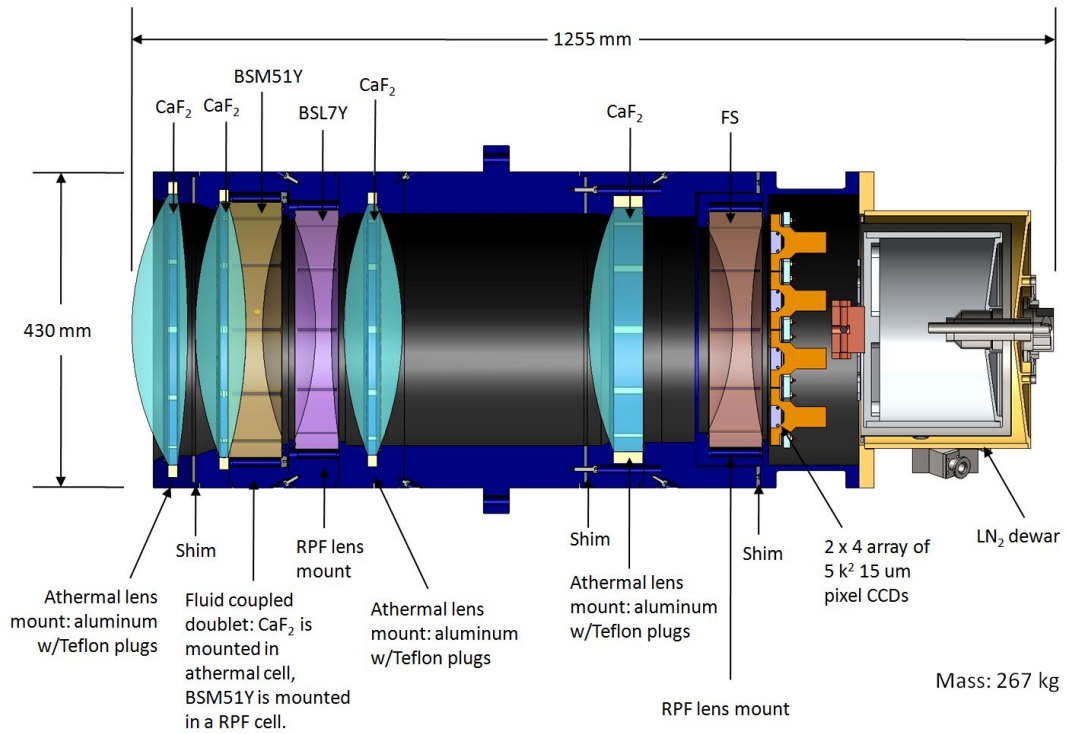


Figure 9 Section view of the blue camera showing the lens arrangement, structure, and cryostat for the detectors.

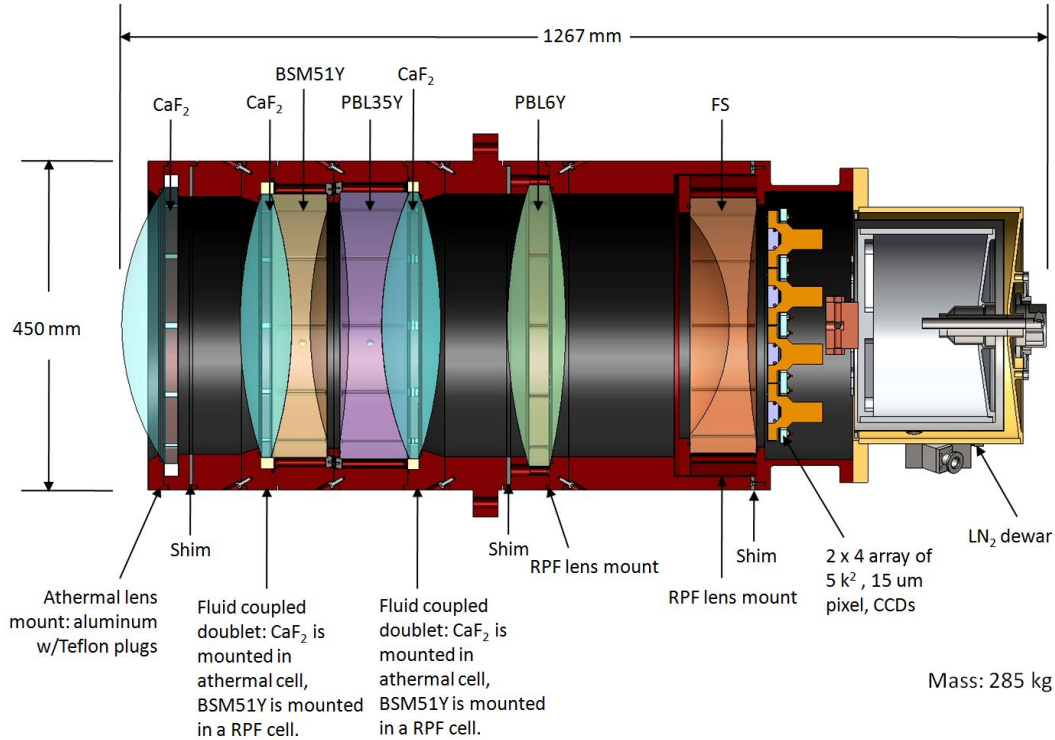


Figure 10 Section view of the red camera showing the lens arrangement, structure, and cryostat for the detectors.

3.5 Detector and dewar

A cryostat holds the detector mosaic for each channel. The CCDs must be operated at a temperature that ensures dark current will not compromise the sensitivity of the observations. Specifically, we expect $\sim 1\text{-}5$ electrons/sec signal from the sky (between emission lines) on an effective pixel that is 0.35 arcsec \times 0.7 arcsec in size on the detector (i.e. A binned pixel set to sample $\sim 1/2$ of a 0.7 arcsec wide slit and 0.7 arcsec along the slit). This binned pixel would contain 6×12 raw pixels (= 72 unbinned pixels). We require that the dark current degrade S/N of the observation by less than 5% relative to no dark current contribution. Therefore, the dark current must be less than 5.4 electrons/pixel/hour (for a raw $15 \mu\text{m}$ pixel). Specifications on E2V CCDs suggest that this level of dark current performance can be achieved at any temperature below ~ 175 K.

We currently advocate using LN₂ cooling. This is not a final decision and we are evaluating new cryo-cooler units that can also be made to work. Experience with some cryo-coolers (cryo-tigers, for example) has not been completely positive. With a MTBF of typically ~ 104 hours and given that we expect to need 2 units per focal plane, we consider the ~ 1 failure per month excessively unreliable and suspect replacement could cause significant maintenance burden on GMT staff. However, we are aware of alternate potential units from SunPower with a demonstrated MTBF of $\sim 100,000$ hours, which would significantly reduce the maintenance and replacement burden. We will continue to evaluate these and similar units as replacements for LN₂ cooling. Note that a drawback to the use of cryo-coolers is that they generate substantial waste heat. The SunPower units, for example, would each dump 265 W of waste heat into the GMT cooling loop; for an additional 4 kW of required heat removal (roughly equal to the amount generated by the entire rest of the instrument).

3.6 GMACS weight summary

The total weight of GMACS has been estimated from the SolidWorks models of the instrument. There are three principle sub-structures:

- Optics Modules: ~3506 kg
- Focal Plane Unit: ~2909 kg
- Door Carriage: ~2934 kg

There are two Optics Modules; the total weight of GMACS will be ~12855 kg.

3.7 Flexure

Gravity loading affects the relative positions of the optical elements of the instrument. Changes in these relative positions as the telescope moves through its complete range of motion will affect instrument performance. Analysis was conducted to quantify these changes as input into an optical sensitivity study. Ultimately, the optical study will provide guidance on the nature of the required flexure compensation mechanism.

Two separate finite element (FE) models were developed. The first model being of the focal plane assembly mounted to its transport wall. The second model consists of one of the optics modules up to and including the flexures that mount it to the telescope GIR. In practice, the focal plane assembly and optics modules would be coupled through the GIR. For the purposes of this conceptual study, the GMACS assemblies are assumed to be mounted to an entirely rigid structure. A reasonable estimate of global (GMACS + GIR) deflections may be made by superimposing the predicted GMACS deflections on top of those predicted for the telescope GIR.

The GMACS flexure study resulted in tables of deflections, rotations, and the direction cosines of normals to optical elements. These results became input to an optical sensitivity analysis (Zemax) that provided the practical implications of the instrument flexure.

To determine the effect of flexure on image motion and image quality, the results from the FEA were imported into Zemax. Given the very tedious nature of transforming global rotations provided by the FEA into relative rotations suitable for Zemax, only the blue channel has been traced at this time, and only for the low-resolution mode. The results are provided in Table 1. Here image shift is provided for the central field point and the central wavelength, in both spectral and spatial. Also provided is the average change in spot size for the entire field, as well as the maximum change for any spot in the field. Results are provided for four cases, i.e. zero gravity zenith pointing, 1G zenith pointing, 1G +65 deg rotation about X, 1G +65 deg rotation about Z. The zero gravity case is of interest strictly from the perspective of image quality, where zero gravity corresponds to the perfectly aligned system.

Table 1 Flexure-induced image shift and image quality for four gravity loading cases: low-res configuration.

Case	X shift (μm) Spatial	Y shift (μm) Spectral	Focus shift (μm)	Avg. RMS \emptyset (μm)	Max. RMS \emptyset (μm)
Zero G	0.0	0.0	0.0	27.8	58.2
1G zenith	-165.2	+19.3	-110.4	29.4	63.9
1G +65° rZ	-231.1	-19.3	-73.1	30.5	66.6
1G +65° rX	-273.5	-14.7	+29.8	29.4	64.8

4. FLEXURE COMPENSATION

Flexure-induced image motion is a common issue for spectrographs mounted at the Cassegrain focus. As the telescope tracks the sky, the gravity vector changes relative to the instrument. Hence, gravity-induced deflections within the spectrograph structure change over time, and alter the position and orientation of the optical elements housed within the structure. These subtle shifts of the optics translate into degradation and motion of the focused images at the camera detector focal plane, which in turn reduces resolution. This problem is particularly acute for large instruments. And for GMACS, the problem is complicated further by the fact that the instrument is comprised by three discrete optomechanical assemblies, i.e. The focal plane assembly, and two separate optics modules.

Flexure compensation schemes built to date fall into one of three categories: 1) passive compensation, 2) open-loop active compensation, and 3) closed-loop active compensation. Passive schemes such as that described by Hileman, et al. (2004)² for GNIRS rely on adjustable cantilevered weights to drive tip and tilt of an optic within the path to compensate for flexure of the entire system. Such a scheme requires accurate knowledge of the expected flexure to ensure the appropriate adjustment degrees of freedom are provided, and tuning once implemented.

The Open-loop active compensation approach, such as that described by Kibrick et al. (2000)³ for the Echelle Spectrograph and Imager (ESI) on Keck II, relies on mathematical predictions or look-up tables to provide corrective adjustment of an optic within the optical train to correct for flexure. On-sky measurements of flexure are used to create the look-up tables, or in the case of analytical prediction, determine the defining constants. On-sky, the ESI flexure control system stabilizes the spectra images to approximately 0.1 pixels (15 μ m pixels), though zero point checks are required nightly.

In the case of closed-loop active compensation, a feedback signal is used to control the motion of a compensating optic. An example of such a closed-loop system is provided by Marshall et al. (2003)⁴ for the Multi-Object Double Spectrograph (MODS) on the Large Binocular Telescope (LBT). Here an infrared laser is traced from the telescope focal plane through the entire optical path to a quadrant detector adjacent to the camera detector. Feedback from the quadrant detector is used to adjust the tip and tilt of the collimator so as to stabilize the position of the spectra on the science detector. Another example of a closed-loop active system is that described by Kibrick et al. (2004)⁵ for the Deep Imaging Multi-Object Spectrograph (DEIMOS) on Keck II. Here fibers are used as light sources to generate a set of artificial objects in the telescope focal plane. Light from these objects is traced through the entire optical path of the instrument and imaged onto two small (600 row x 1200 column) CCD detectors adjacent to the science CCD mosaic. A CuAr light source is used to illuminate the fibers. The CuAr lamp provides a rich spectrum with broad wavelength coverage. Motion of the fiber source images are measured during an exposure and those measurements are used as feedback to a tilt mirror and the dewar translation stage, which combined, are used to adjust the location of the spectra on the mosaic. Both the MODS and the DEIMOS flexure control systems provide of order 0.1 pixel flexure stability during an observation.

As of this writing the flexure compensation scheme for GMACS is still being evaluated. The current thinking is to have a hybrid system consisting of an open-loop system and a closed-loop system. The open-loop system would use actuation of the tent mirrors to provide tip/tilt/flexure correction of the focal plane assembly relative to the optics modules. A mathematical model or lookup table would be generated from calibration data taken on-sky at discrete elevation and rotator angles of the telescope. These data would be used to determine the tip and tilt of each tent mirror as a function of telescope pointing. For the closed-loop system we would adopt a system very similar to that used by DEIMOS whereby four fiber sources would project artificial objects through windows in the slit mask and image onto four small CCDs located along the top and bottom (spatial direction) edge of the science mosaic. The sources along a given edge would be separated in the spectral direction so as to provide a broad sampling of image motion across the mosaic (a source at roughly each corner of the mosaic). Each fiber would be fed by a CuAr lamp that is filtered to provide only a minimum number of spectral lines (to mitigate stray light). The flexure correction CCDs would be parfocal with the science mosaic and the entire ensemble of detectors would be mounted on a hexapod inside the camera dewar. Feedback from centroids of the fiber sources would be used to determine image motion in X (row), Y (column), and rotation. Furthermore, we believe that we could measure focus of the mosaic if each fiber source were actually five fibers, each slightly offset from the other, such that the middle fiber is parfocal with the telescope focus, and of the remaining two, one pair is in front of focus and the other pair behind focus. Thus each fiber bundle produces five PSFs for each spectral line provided by the CuAr lamp. Adjusting the science mosaic in piston such that the center PSF is minimized achieves focus. We envision that this closed loop control would provide updates several times per minute.

REFERENCES

-
- [1] DePoy, D. L., Allen, R., Barkhouser, R., Boster, E., Carona, D., Harding, A., Hammond, R., Marshall, J. L., Orndorff, J., Papovich, C., Prochaska, T., Eheault, J. P., Smee, S., Sheckman, S., Villanueva, S., "GMACS: a wide field, moderate resolution, optical spectrograph for the Giant Magellan Telescope," Proc. SPIE 8446, (2012)

-
- [2] Hileman, E. A., Elias, J., Joyce, R., Probst, R. Liang, M., Pearson, E., "Passive compensation of gravity flexure in optical instruments", Proc. SPIE 5495, pp. 622-635, (2004).
 - [3] Kibrick, R. I., Miller, J. S., Nelson, J. E., Radovan, M. V., Sheinis, A. I., Sutin, B. M., "Active flexure compensation software for the echellette spectrograph and imager on Keck II," Proc. SPIE 4009, pp. 262-273, (2000).
 - [4] Marshall, J. L., Atwood, B., Byard, P. L., DePoy, D. L., O'Brien, T. P., Pogge, R. W., "An image motion compensation system for the Multi-Object Double Spectrograph," Proc. SPIE 4841, pp. 1273-1279, (2003).
 - [5] Kibrick, R. I., Allen, S. L., Clarke, De A., Faber, S. M., Phillips, A. C., Wirth, G. D., "The DEIMOS Flexure compensation system: overview and operational results," Proc. SPIE 5492, pp. 799-810 (2004).